THE JOURNAL OF BIOLOGICAL CHEMISTRY Vol. 278, No. 45, Issue of November 7, pp. 44593–44599, 2003
Printed in U.S.A.

Crystal Structure of Human Cholesterol Sulfotransferase (SULT2B1b) in the Presence of Pregnenolone and 3′-Phosphoadenosine 5′-Phosphate

RATIONALE FOR SPECIFICITY DIFFERENCES BETWEEN PROTOTYPICAL SULT2A1 AND THE SULT2B1 ISOFORMS*

Received for publication, July 30, 2003, and in revised form, August 14, 2003
Published, JBC Papers in Press, August 14, 2003, DOI 10.1074/jbc.M308312200

Karen A. Lee‡§, Hirotoshi Fuda¶, Young C. Lee¶, Masahiko Negishi§, Charles A. Strott¶, and Lars C. Pedersen‡‖

From the ‡Laboratory of Structural Biology and the §Pharmacogenetic Section, Laboratory of Reproductive and Developmental Toxicology, National Institute of Environmental Health Sciences, National Institutes of Health, Research Triangle Park, North Carolina 27709, and the ¶Section on Steroid Regulation, Endocrinology and Reproduction Research Branch, NICHD, National Institutes of Health, Bethesda, Maryland 20892-4510

The gene for human hydroxysteroid sulfotransferase (SULT2B1) encodes two peptides, SULT2B1a and SULT2B1b, that differ only at their amino termini. SULT2B1b has a predilection for cholesterol but is also capable of sulfonating pregnenolone, whereas SULT2B1a preferentially sulfonates pregnenolone and only minimally sulfonates cholesterol. We have determined the crystal structure of SULT2B1a and SULT2B1b bound to the substrate donor product 3′-phosphoadenosine 5′-phosphate at 2.9 and 2.4 Å, respectively, as well as SULT2B1b in the presence of the acceptor substrate pregnenolone at 2.3 Å. These structures reveal a different catalytic binding orientation for the substrate from a previously determined structure of hydroxysteroid sulfotransferase (SULT2A1) binding dehydroepiandrosterone. In addition, the amino-terminal helix comprising residues Asp[19] to Lys[26], which determines the specificity difference between the SULT2B1 isoforms, becomes ordered upon pregnenolone binding, covering the substrate binding pocket.

Sulfonation of endogenous compounds and xenobiotics is catalyzed by a large group of enzymes called sulfotransferases. These enzymes catalyze the transfer of a SO_3 group from PAPS,[1] the universal sulfonate donor molecule, to an acceptor group of various substrates. Cytosolic sulfotransferases sulfonate small molecules such as hormones, neurotransmitters, bioamines, and therapeutic drugs (1, 2). Hydroxysteroid sulfotransferases sulfonate the 3-hydroxy group of steroids and are part of the superfamily of cytosolic sulfotransferases that includes phenol (aryl) and amine sulfotransferases. The prototypical human hydroxysteroid sulfotransferase SULT2A1 readily sulfonates dehydroepiandrosterone (DHEA) but also has a broad substrate predilection (3). Recently, two human hydroxysteroid sulfotransferases, SULT2B1a and SULT2B1b, have been shown to be encoded by the same gene but differ at the amino terminus by 8 and 23 amino acids, respectively, as a result of an alternative exon 1 (4). The SULT2B1a isoform avidly sulfonates pregnenolone, whereas sulfonation of cholesterol is minimal. In contrast, the SULT2B1b isoform preferentially sulfonates cholesterol with greater efficiency and, to a lesser extent, pregnenolone (5). Although both isoforms are capable of sulfonating DHEA, they do so with relatively low efficiencies (3).

Differential expression patterns of SULT2B1a and SULT2B1b in organ systems, particularly the skin and brain, in association with their respective substrate preferences reveal potential physiological implications for the sulfonated product. SULT2B1b, now recognized as a cholesterol sulfotransferase, is quantitatively the predominant hydroxysteroid sulfotransferase expressed in human skin. Cholesterol sulfate has been recognized to be essential in skin development as a regulatory molecule in human keratinocyte differentiation and creation of the barrier (6–9). The human fetal brain appears to only express the SULT2B1a isoform (10), which is consistent with the evidence that the brain and spinal cord in mouse almost exclusively express SULT2B1a (11). Pregnenolone sulfate, which is most efficiently produced by SULT2B1a, is now acknowledged as an essential neurosteroid that modulates neurotransmitters such as γ-aminobutyric acid type A, *N*-methyl-D-aspartate, and Sigma 1 (11–16).

Although the SULT2A1 and SULT2B1 isozymes are ~37% identical in amino acid sequence, the SULT2B1 isoforms have extended amino- and carboxyl-terminal ends that are absent in the SULT2A1 isozyme (5). Previous studies showed that removal of the 52 amino acid carboxyl-terminal end that is common to both SULT2B1 isoforms has no effect on catalytic activity of either isoform (5). Removal of the 8-residue amino-terminal end that is unique to SULT2B1a has no significant effect on catalytic activity; however, removal of the 23-residue amino-terminal end that is unique to SULT2B1b abolishes catalytic activity for cholesterol but not pregnenolone (5). Full wild-type activity of SULT2B1b for cholesterol can be retained if only the first 18 amino acids are deleted (5). This finding suggests that residues [19]DISEI[23] are responsible for the ability of SULT2B1b to sulfonate cholesterol. Thus, the difference in substrate specificity appears to lie at the unique amino terminus of the SULT2B1 isoforms.

* The costs of publication of this article were defrayed in part by the payment of page charges. This article must therefore be hereby marked "*advertisement*" in accordance with 18 U.S.C. Section 1734 solely to indicate this fact.

‖ To whom correspondence should be addressed: Laboratory of Structural Biology, NIEHS, National Institutes of Health, Research Triangle Park, NC 27709. Tel.: 919-541-0444; Fax: 919-541-7880; E-mail: pederse2@niehs.nih.gov.

[1] The abbreviations used are: PAPS, adenosine 3′-phosphate 5′-phosphosulfate; PAP, 3′-phosphoadenosine 5′-phosphate; SULT, sulfotransferase; DHEA, dehydroepiandrosterone; CHES, 2-(cyclohexylamino)ethanesulfonic acid; r.m.s., root mean square; EST, estrogen sulfotransferase; E2, estradiol-17β.

TABLE I
Crystallographic data statistics

Data set	2b1a	2b1b	2b1b + pregnenolone	2b1b + DHEA
Data Collection				
Unit cell dimensions	$a = b = 75.26$; $c = 252.27$ $\alpha = \beta = \gamma = 90°$	$a = b = 75.72$; $c = 252.08$ $\alpha = \beta = \gamma = 90°$	$a = b = 75.96$; $c = 253.62$ $\alpha = \beta = \gamma = 90°$	$a = b = 75.859$; $c = 253.8$ $\alpha = \beta = \gamma = 90°$
Resolution (Å)	25–2.9	50–2.4	50–2.3	50–2.5
Space group	$P4_12_12$	$P4_12_12$	$P4_12_12$	$P4_12_12$
No. of observations	105,367	71,042	174,703	141,095
Unique reflections	29,928	26,998	32,282	25,505
R_{sym} (%) (last shell)[a]	8.1 (59.8)	11.3 (37.5)	5.8 (31.2)	11.9 (37.7)
I/σI (last shell)	12.1 (2.1)	25.3 (2.0)	14.3 (3.2)	25.9 (3.5)
Mosaicity	1.1	0.6	0.5	0.8
Completeness (%) (last shell)	99.0 (98.5)	90.3 (78.2)	95.4 (78.4)	96.0 (86.8)
Refinement statistics				
R_{cryst} (%) (last shell)[b]	24.9 (41.0)	21.7 (31.8)	21.1 (31.0)	22.1 (31.6)
R_{free} (%) (last shell)[b]	26.9 (41.0)	23.7 (35.4)	22.5 (30.5)	25.2 (32.5)
No. of waters	7	78	119	63
R.m.s. deviation from ideal values				
Bond length (Å)	0.010	0.008	0.011	0.008
Bond angle (°)	1.5	1.4	1.4	1.3
Dihedral angle (°)	22.0	22.5	21.9	21.8
Improper angle (°)	1.8	0.9	0.9	0.9
Mean B value (Å^2)	46.3	51.4	41.9	47.8
Mean B value of ligand (Å^2)	35.6 (PAP)	36.7 (PAP)	28.9 (PAP) 46.0 (PREG)	35.6 (PAP) 48.9 (DHEA)
Ramachandran statistics				
Most favored region (%)	82.1	88.8	92.0	88.7
Additional allowed (%)	17.0	11.2	8.0	11.3
Generously allowed (%)	0.9	0.0	0.0	0.0
Disallowed (%)	0.0	0.0	0.0	0.0
Protein Data Bank code	1Q1Q	1Q1Z	1Q20	1Q22

[a] $R_{sym} = \Sigma(|I_i - \langle I \rangle|)/\Sigma(I_i)$ where I_i is the intensity of the ith observation and $\langle I \rangle$ is the mean intensity of the reflection.
[b] $R_{cryst} = \Sigma||F_o| - |F_c||/\Sigma|F_o|$ calculated from working data set. R_{free} is calculated from 5% of data randomly chosen not to be included in refinement.

To better understand the nature of the substrate specificity differences among SULT2A1, SULT2B1a, and SULT2B1b, we have solved the x-ray crystal structures of SULT2B1a and an active truncated version of SULT2B1b (Asp^{19}-Asp^{312}) in the presence of PAP, the substrate donor product, as well as the structure of SULT2B1b in the presence of PAP and the acceptor substrate pregnenolone. These structures reveal a different orientation of acceptor substrate binding for SULT2A1 and the SULT2B1 isoforms and suggest a possible role for the unique amino terminus of SULT2B1b in determining substrate specificity for cholesterol.

EXPERIMENTAL PROCEDURES

Expression and Purification of SULT2B1a and SULT2B1b—SULT2B1a cDNA (GenBank™ accession number U92314) was cloned into the pGEX-6P-3 vector (Amersham Biosciences) as previously described to create a glutathione *S*-transferase-SULT2B1a fusion protein (5). This construct was then used to transform *Escherichia coli* BL21-CodonPlus(DE3)-RIL cells (Stratagene). The truncated form of SULT2B1b (Asp^{19}-Asp^{312}) used for the crystallographic studies was cloned from the previously described pGEX-6P-3 glutathione *S*-transferase-SULT2B1b fusion plasmid containing the full-length SULT2B1b cDNA (GenBank™ accession number U92315) using the upstream primer 5′-CCGAATTCCGACATCTCGGAAATCAGCCAGAAG-3′ and the downstream primer 5′-ATAGTTTAGCGGCCGCTCAGTCTTCATC-CCAGGGGAAGGTCGG-3′ (5). The PCR product was cloned into the pGEX-4T-3 vector (Amersham Biosciences) using *Eco*RI and *Not*I restriction sites. DNA sequencing identified appropriate clones. The corresponding construct was transformed into *E. coli* BL21-CodonPlus(DE3)-RIL cells.

SULT2B1a fusion protein was expressed overnight in 2× YT (16 g of bacto-tryptone, 10 g of bacto-yeast extract, 5 g of NaCl, and 5 ml of 1 M NaOH in 1 liter) media at 22 °C on a shaker after induction with isopropyl-1-thio-β-D-galactopyranoside at a final concentration of 0.2 mM. Cells were pelleted, resuspended in the lysis buffer (50 mM Hepes, pH 7.5, and 350 mM NaCl), sonicated on ice, and spun down. Soluble protein was loaded onto glutathione-Sepharose 4B resin. The resin was washed extensively in batch with lysis buffer plus 1 mM EDTA and 1 mM dithiothreitol. The full-length SULT2B1a enzyme was eluted from the resin by PreScission protease (Amersham Biosciences) digestion, and the protein was concentrated to 15 mg/ml and then dialyzed overnight against 20 mM Hepes, pH 7.5, and 100 mM NaCl. Protein was loaded onto a PAP-agarose column but did not bind. The flow-through was then loaded onto a Q-Sepharose column and eluted with a salt gradient from 100 mM to 1.0 M NaCl. The eluted protein was then concentrated to 13 mg/ml and dialyzed against 20 mM Hepes, pH 7.5, and 100 mM NaCl. PAP was then added to the concentrated protein for a final concentration of 4 mM.

The SULT2B1b fusion protein was expressed, and cells were disrupted using a very similar protocol but with a lysis buffer containing 50 mM Tris, pH 7.5, 500 mM NaCl. Soluble protein was loaded onto glutathione-Sepharose 4B resin and extensively washed in lysis buffer and 0.5 mM PAP. The pure SULT2B1b enzyme was then eluted by thrombin digestion. PAP was added to the eluted protein for a final concentration of 1 mM to increase the protein solubility. The protein then was concentrated to ~15 mg/ml and run over a Superdex 75 HR 10/30 column with 25 mM Tris, pH 7.5, and 100 mM NaCl. The fractions corresponding to SULT2B1b were concentrated to 23 mg/ml, and PAP was added for a final concentration of 4 mM.

Protein Crystallization—Crystals of SULT2B1a were grown by the hanging drop vapor diffusion method by mixing 2 μl of prepared SULT2B1a with 2 μl of reservoir solution containing 0.8–1.0 M sodium tartrate, 0.2 M Li_2SO_4, and 0.1 M CHES, pH 9.0. Crystals were transferred in four steps of increasing sodium tartrate and ethylene glycol into 1.5 M sodium tartrate, 15% ethylene glycol, 40 mM Li_2SO_4, 4 mM PAP, and 80 mM CHES, pH 9.0, and then flash-cooled in a stream of nitrogen gas cooled to −180 °C for data collection. Attempts to co-crystallize full-length SULT2B1a in the presence of pregnenolone resulted in crystals, but no substrate was observed in the acceptor substrate binding pocket. In addition, attempts to soak pregnenolone into the crystal also failed. However, it was discovered that a molecule of CHES from the buffer was binding with the sulfate group interacting with Gln^{170} and Tyr^{29} in a competitive manner to the acceptor substrate in the binding pocket. Attempts to co-crystallize the complex in Tris buffer did not result in diffraction quality crystals.

Crystals of SULT2B1b were obtained using the hanging drop method by mixing 2 μl of prepared protein with 2 μl of reservoir solution containing between 0.55 and 0.8 M sodium citrate and 0.1 M imidazole

TABLE II
Catalytic activity of SULT2B1b construct

Protein	Cholesterol	Pregnenolone
	nmol/min/mg	*nmol/min/mg*
Full-length	9.4 ± 0.45	2.1 ± 0.09
Asp^{19}-Asp^{312}	6.1 ± 0.15	7.9 ± 0.17

at pH 8.0–8.5. For co-crystallization attempts, 1 mM pregnenolone, 1 mM DHEA, saturated cholesterol (<1 mM), and saturated 25-hydroxycholesterol (<1 mM) were added to the protein solution of different hanging drops. These crystals were transferred in four steps of increasing sodium citrate and ethylene glycol concentrations into the cryosolution consisting of 1.0 M sodium citrate, 0.1 M imidazole, pH 8.0, 50 mM NaCl, 1 mM PAP between 1 mM and saturated acceptor substrate, and 10% ethylene glycol. Crystals were flash-cooled directly into liquid nitrogen and then transferred into a stream of nitrogen gas cooled to −180 °C. Electron density was visible for the pregnenolone and DHEA data sets. The 25-hydroxycholesterol data set did not produce electron density for the substrate; however, it diffracted to higher resolution than any apocrystals tried, therefore it is used as the apodata set.

Data Collection and Refinement—The SULT2B1b data set collected in the presence of pregnenolone was collected on a MARCCD area detector system at the Southeast Regional Collaborative Access Team beamline 22 at Advanced Photon Service. All of the other data sets were collected on a Rigaku RU3H rotating anode generator with a Raxis4 area detector and MSC blue mirrors (Table I). All of the diffraction data were processed using HKL2000 (17). The phase problem for the SULT2B1a data set was solved by molecular replacement using the program AMoRe (18) from the CCP4 package (19) with the x-ray crystal structure of SULT2A1 solved in the presence of PAP and with no acceptor substrate as the starting model (20). This model was refined at 2.9-Å resolution using iterative cycles of model building with the program O (21), and torsion angle simulated annealing, energy minimization, and individual B-factor refinement using the program CNS (22). The model of SULT2B1a was then used to refine the structure of SULT2B1b in the presence of pregnenolone at 2.3 Å in a similar fashion. This structure was used as the starting model to solve the structures of the apo and DHEA data sets of SULT2B1b. The quality of the models was checked using PROCHECK (23). Ordered residues for the SULT2B1a structure are Leu^{12}-Leu^{95} and Ser^{103}-Glu^{296}. Ordered residues for the SULT2B1b structure with pregnenolone bound are Ser^{18} (from the thrombin cleavage site) and Asp^{19}-Glu^{311}. Ordered residues for the SULT2B1b structure with DHEA are Ser^{18}, Asp^{19}-Asp^{115}, and Ser^{118}-Glu^{311}. The ordered residues for the SULT2B1b structure with no acceptor substrate present are Leu^{27}-Asp^{115} and Pro^{119}-Glu^{311}.

Sulfotransferase Assay—Sulfotransferase activity of truncated SULT2B1b was determined using radiolabeled cholesterol and pregnenolone according to a previously reported procedure (5). 20-μl reaction volumes contained 0.4 μg/tube SULT2B1b and either cholesterol or pregnenolone at 5 μM. Reactions were carried out at 37 °C for 5 min. This construct was shown to have two-thirds the activity for cholesterol and four times the activity for pregnenolone as the full-length protein (Table II). Activity for the full-length SULT2B1a used in these experiments has been reported previously (5).

RESULTS

Overall Description—The crystal structures of full-length SULT2B1a and the construct Asp^{19}-Asp^{312} of SULT2B1b with PAP and no acceptor substrate bound are for all intents and purposes identical. For SULT2B1a, the amino-terminal 11 residues and the carboxyl-terminal 52 residues (proline-rich region) are disordered. For SULT2B1b, residues Asp^{13}-Lys^{26} are disordered. Therefore, the sequences of the ordered residues are identical. Because the structure of SULT2B1b is a higher resolution structure, the discussion of the structures will focus on the SULT2B1b structures.

The overall structure of SULT2B1b is that of the classical cytosolic sulfotransferase fold consisting of an α/β motif comprised of a central 5-stranded parallel β-sheet (Fig. 1). Superposition to other cytosolic sulfotransferases reveals a r.m.s. of 1.3 Å for 272 structurally equivalent Cαs to human estrogen sulfotransferase (EST) (24) and 1.5 Å for 263 structurally equivalent Cαs to SULT2A1 (25). As might be expected, residues surrounding the PAPS binding site are highly conserved among the cytosolic sulfotransferases with the major structural and sequence differences existing around the hydrophobic acceptor substrate binding pocket.

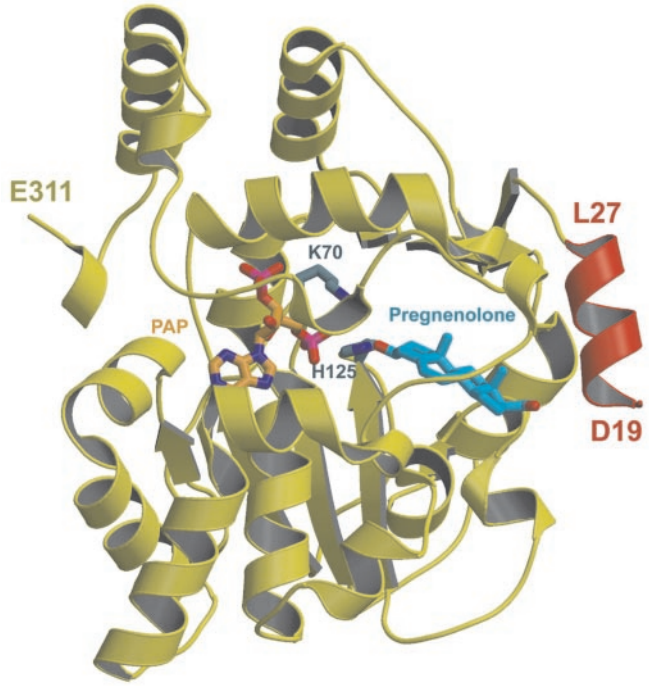

FIG. 1. **Ribbon diagram of SULT2B1b co-crystallized in the presence of substrate donor product PAP (*orange*) and the acceptor substrate pregnenolone (*light blue*).** The amino-terminal helix (*red*) is disordered in the SULT2B1b + PAP complex but becomes ordered upon acceptor substrate binding. Catalytic residues Lys^{70} and His^{125} are also pictured (*cadetblue*). This figure was created using MOLSCRIPT and Raster3D (31, 32).

PAP Binding—The loop connecting the first strand of the central β-sheet with the first helix forms the PSB-loop (residues ^{67}TYPKSGT^{73}) (26). This loop is similar in structure to the P-loop motifs found in many protein kinases and is involved in binding the 5′-phosphate of PAPS (or PAP) (27). A number of residues from the PSB-loop form interactions with the 5′-phosphate of PAP (Fig. 2*a*). Backbone amide nitrogens from Ser^{71} (3.1 Å), Gly^{72} (3.1 Å), and Thr^{73} (2.8 Å) as well as the hydroxyl oxygen of Thr^{73} (2.5 Å) are all within hydrogen-bonding distance to the oxygen atom O4P of the 5′-phosphate. The O5P oxygen of the 5′-phosphate is in position to form hydrogen bonds with both the backbone amide nitrogen (2.9 Å) and the hydroxyl oxygen (2.8 Å) of Thr^{74}. The amine nitrogen from highly conserved Lys^{70} is within hydrogen-bonding distance (3.0 Å) to the oxygen atom O6P of the 5′-phosphate. From a previously solved structure of human EST in complex with PAPS, it has been shown that this oxygen is the bridging oxygen between the 5′-phosphate and the sulfuryl moiety (Fig. 2*b*) (24).

A number of residues are also involved in binding the 3′-phosphate. Backbone amide nitrogens from Lys^{275} (2.8 Å) and Gly^{276} (2.9 Å) are in position to bind the O2P phosphate oxygen, whereas the O3P phosphate oxygen is within hydrogen-bonding distances to nitrogen atom NH_2 of Arg^{274} (3.1 Å) and atom NH_2 of Arg^{147} (3.1 Å). The O1P oxygen of the 3′-phosphate is 3.1 Å from nitrogen atom NE of Arg^{274} and is also 2.8 Å from the hydroxyl oxygen of the highly conserved residue Ser^{155}.

The adenine group of PAP is found sandwiched between two aromatic residues in a parallel ring-stacking orientation with Trp^{75} and anti-parallel ring-stacking orientation with Phe^{246}.

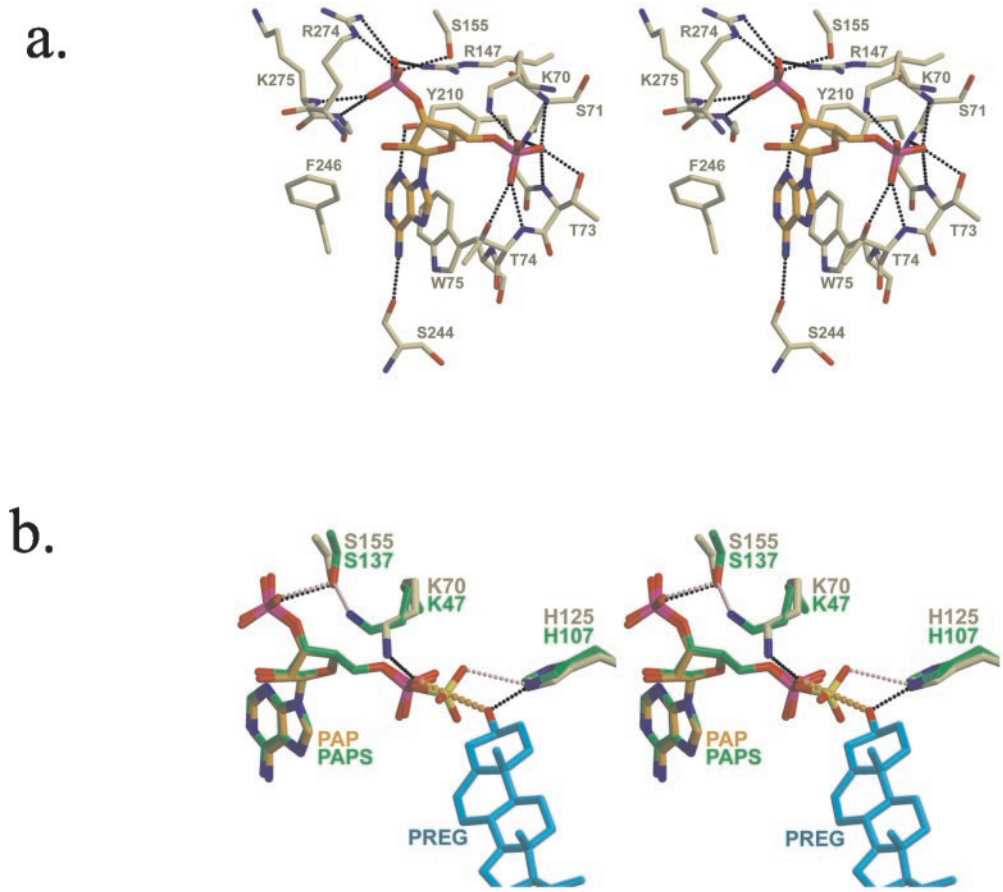

FIG. 2. *a*, stereodiagram of the PAPS binding site of SULT2B1b with PAP (*orange*) bound. Hydrogen bonds are shown by *dashed black lines*. *b*, superposition of the active sites of human EST with PAPS bound (*green*) and SULT2B1 (*khaki*) with PAP (*orange*) and pregnenolone (*light blue*) bound (based on superposition of PSB-loops). The catalytic Ser^{155}, Lys^{70}, and His^{125} are shown pictured with hydrogen bonds (*black dashed lines*) to the bridging oxygen of PAP and the acceptor O3 oxygen of pregnenolone. Hydrogen bonds between human EST and PAPS are shown as *pink dashed lines*. The sulfur atom from PAPS is shown in *yellow*. A *dashed orange line* has been drawn from the acceptor O3 oxygen of the pregnenolone molecule to the leaving group bridging oxygen of PAP. This line goes right through the sulfur supporting the proposed S_N2-like in-line displacement mechanism. This figure was created using MOLSCRIPT and Raster3D (31, 32).

Atom N3 of the adenine is hydrogen bound to the phenolic hydroxyl of Tyr^{210} (2.8 Å), and the N6 amine nitrogen is 2.9 Å from the carbonyl oxygen of Ser^{244}.

Substrate Binding—The crystal structures of SULT2B1b in the presence of PAP and acceptor substrates pregnenolone or DHEA reveals that these two similar compounds, which differ at the C17 carbon side chain, bind in identical positions and orientations (Fig. 3, *a–c*). The substrate binding site is highly hydrophobic. There is only one hydrogen bond (2.7 Å) made between the protein and substrate that is between the O3 acceptor hydroxyl off the C3 carbon and atom NE2 of His^{125}, the proposed catalytic base. Residues found lining the hydrophobic acceptor binding pocket near the A ring of the steroid substrates other than His^{125} are Phe^{272}, Tyr^{159}, Gln^{165}, Tyr^{44}, and Trp^{103}. The aromatic side chain of Trp^{103} is stacked parallel to that of the steroids A and B rings (Fig. 3*a*). Residues found lining the pocket near the B and C rings are Tyr^{257}, Leu^{260}, and Thr^{106}. Finally, residues found lining the opening of the binding pocket at the surface of the protein near the D ring of the steroid are Trp^{98}, Val^{108}, Leu^{43}, Leu^{264}, and Ile^{20}. Interestingly, Ile^{20} resides on the amino-terminal helix comprised of residues Asp^{19} to Lys^{26}, which is only ordered upon substrate binding and is required for cholesterol activity. In both the SULT2B1a and SULT2B1b structures with no acceptor substrate, the first ordered residue is the leucine equivalent to that of Leu^{27} in SULT2B1b.

DISCUSSION

Catalytic Mechanism—Based on the crystal structure of mouse EST with PAP and estradiol-17β (E2) bound, it has previously been suggested that sulfotransferases proceed by an S_N2-like in-line displacement reaction mechanism (27). The position of pregnenolone binding in SULT2B1b places the acceptor hydroxyl 4.3 Å away from the position of the bridging oxygen between the 5′-phosphate and the sulfuryl group in PAPS. Superposition of PAPS from the human EST + PAPS structure on to the SULT2B1b active site positions the sulfur atom of PAPS 2.6 Å from the acceptor hydroxyl in line with the acceptor hydroxyl and the bridging oxygen from the leaving group PAP (Fig. 2*b*) (24). Thus, this geometry supports the in-line displacement mechanism.

In such a reaction mechanism for SULT2B1b, conserved His^{125} could serve as a general base to help deprotonate the acceptor hydroxyl and conserved Lys^{70} could help to reduce the negative charge build up on the bridging oxygen between the leaving group PAP and the sulfuryl group of PAPS. Interestingly, in the structure of PAPS bound to human EST, residues equivalent to conserved Ser^{155}, which interacts with the 3′-phosphate of PAP, and Lys^{70} form a hydrogen bond (24). However, in the transition state and PAP bound states, the lysine side chain undergoes a conformational change and interacts with the bridging oxygen between the 5′-phosphate and the sulfuryl group to help facilitate sulfuryl transfer (24,

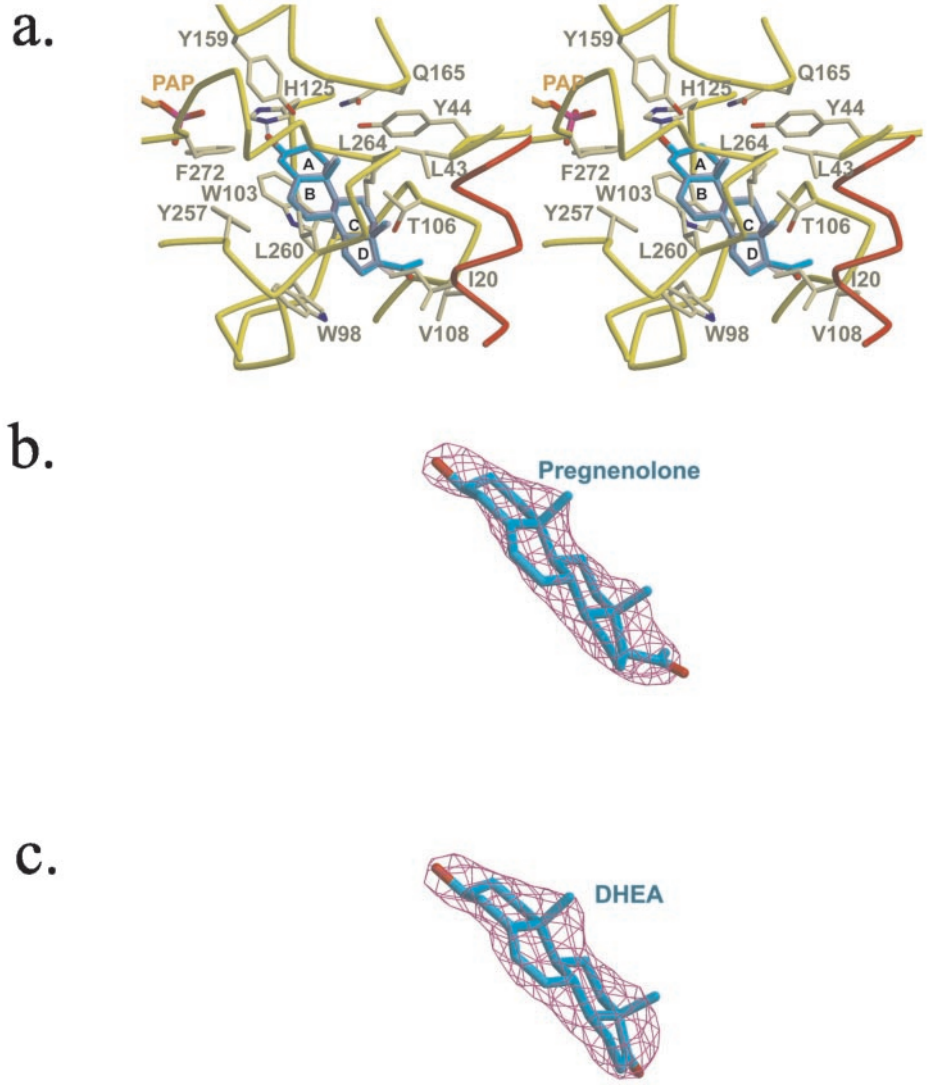

FIG. 3. *a*, stereodiagram of the hydrophobic acceptor substrate binding site with pregnenolone bound (*light blue*) and the amino-terminal helix is shown in *red*. The position of the DHEA (*light purple*) molecule is superimposed into the active site based on superposition of Cα atoms between the two structures. Residues within 4.4 Å are pictured in *khaki* with the backbone trace in *yellow*. The hydrogen bond between the catalytic histidine 125 and the O3 oxygen of the pregnenolone is shown by a *gray line*. *b* and *c*, pictured is the electron density from simulated annealing $F_o - F_c$ omit maps contoured at 3σ from the refinement of the data set with pregnenolone bound (*b*) and DHEA bound (*c*). This figure was created using MOLSCRIPT and Raster3D (31, 32).

28). Thus, residue Ser^{155} may participate not only in substrate donor binding but may help inhibit hydrolysis of PAPS by interacting with the lysine in the absence of acceptor substrate (Fig. 2*b*).

Comparision to Human EST and SULT2A1—Although the overall fold of the SULT2B1 isoforms is very similar to that of other cytosolic sulfotransferases, there is a striking difference in the position of the acceptor substrates (Fig. 4). Three other cytosolic sulfotransferases that have been solved in the presence of their presumed physiological substrates are human EST and mouse EST in the presence of E2 and human SULT2A1 in the presence of DHEA (24, 25, 27). Interestingly, DHEA is found in two different competitive orientations in the active site of SULT2A1 (25). One site positions the acceptor hydroxyl in the same position as that of E2 in the human EST structure, and the molecule extends out toward the surface of the protein in the same direction and position as E2 but rotated by approximately 30° with respect to an imaginary axis running the length of the molecules. This is believed to be the catalytically relevant binding orientation of DHEA (25). The other position of the DHEA molecule binds such that the C3 carbon only differs in position by 1.1 Å; however, the molecule has shifted such that the O17 ketone oxygen has moved 7.4 Å from that of the catalytic binding position resulting in an approximate 45° angle difference in binding. This positions the acceptor hydroxyl 2.2 Å away from the catalytic position, no

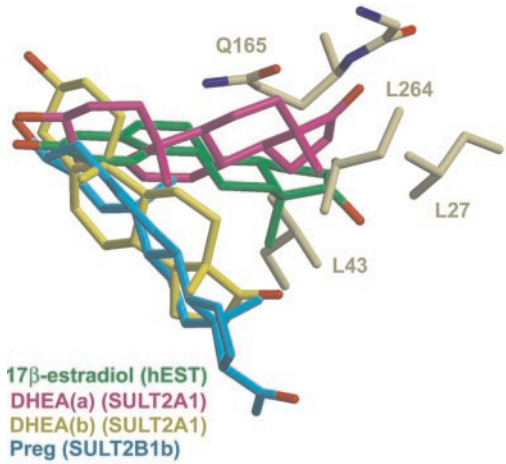

FIG. 4. **Superposition of acceptor substrates from human EST and SULT2A1 onto the active site of SULT2B1 with pregnenolone bound (17β-estradiol (*green*) from the crystal structure of human EST (24), alternate binding conformations of DHEA to SULT2A1, catalytic (*purple*), and substrate inhibition site (*yellow*)).** Superpositions are based on all of the structurally equivalent Cα atoms. Residues from the SULT2B1b (*khaki*) that are likely to form steric clashes if pregnenolone bound in the same catalytic binding orientation as 17β-estradiol to human EST or DHEA to SULT2A1 are shown. This figure was created using MOLSCRIPT and Raster3D (31, 32).

longer in line with the position of the leaving group PAP of PAPS. Thus, this position has been suggested to be involved in substrate inhibition. Interestingly, the catalytic binding position of pregnenolone and DHEA in the SULT2B1b structures is in the same position but a different orientation as the substrate inhibition site of SULT2A1 (Fig. 4). However, in the case of SULT2B1b, the acceptor hydroxyl is in the correct position and orientation for catalysis (Fig. 2*b*). In addition, the pregnenolone and DHEA are rotated approximately 170° along the imaginary long axis of the molecule with respect to DHEA binding in the substrate inhibition site in SULT2A1.

Structural difference at the opening of the binding pocket suggest that residues Gln^{165}, Leu^{43}, Leu^{27}, and Leu^{264} of SULT2B1b would form steric clashes with the D ring of a steroid if it were bound in the catalytic orientation as E2 in human EST and DHEA in SULT2A1 (Fig. 4). Perhaps the most striking structural difference in the overall fold in this protein is the position of the amino-terminal helix of SULT2B1b with respect to human EST and SULT2A1. Structural similarities between the proteins begin at residue Glu^{30} of SULT2B1b. In the acceptor substrate bound structure of SULT2B1b, the amino-terminal helix runs across the opening of the acceptor substrate binding pocket positioning itself between loops containing residues Leu^{259} to Ser^{263} and Thr^{106} to Val^{108}, effectively burying the substrate in the hydrophobic binding site (Fig. 3*a*).

Substrate Specificity of SULT2B1a and SULT2B1b—Previously, it has been suggested that the specificity difference for cholesterol and pregnenolone between SULT2B1a and SULT2B1b could be traced to the unique amino-terminal residues ^{19}DISEI^{23} (5). The results from alanine-scanning mutagenesis of the ^{19}DISEI^{23} region reveal that only the I20A and I23A mutants knocked out cholesterol-sulfonating activity. It was then shown that this activity could be partially restored by replacement with a conservative substitution such as leucine (5). The position of Ile^{20} and Ile^{23} are such that they lie on the same side of the helix facing on the inside of the hydrophobic pocket, whereas residues Ser^{21} and Glu^{22} are solvent-exposed. Interestingly, the residues corresponding to ^{19}DISEI^{23} of SULT2B1b are ^{4}PPPFH^{8} in SULT2B1a. With three prolines in a row, it is unlikely that these residues are able to form a α-helix and therefore would be unable to cover the opening to the substrate binding pocket in the same manner as is seen in the SULT2B1b structure. Although we do not have a crystal structure of SULT2B1b with cholesterol bound yet, the position of pregnenolone is such that the O20 ketone is only 3.4 Å from atom CD1 of Ile^{20} and the C21 atom is 6.0 Å from atom CD1 of Ile^{23}. Thus, these residues may be in position to form positive van der Waal's interactions with the longer side chain of the C17 atom of cholesterol. However, slight conformational changes of the protein may be necessary to accommodate the longer side chain of cholesterol.

Alternatively, it is possible that Ile^{20} may form positive van der Waal's interactions with the hydrophobic side chain of cholesterol, whereas the role of Ile^{23} is to form positive van der Waal's interactions with residues Leu^{27}, Gly^{42}, and Leu^{43} locking the helix in place. Neither interaction alone may be enough to bind the helix in the present orientation upon substrate binding, but when both are present the helix can lock down in position over the active site to bind the hydrophobic cholesterol molecule. To better understand the possible binding position of the cholesterol side chain, coordinates of cholesterol were taken from the structures of cholesterol bound to β-cryptogein (29) and bound to nuclear receptor retinoic acid-related orphan receptor α ligand binding domain (30) and superimposed on the pregnenolone molecule bound to SULT2B1b. In these superpositions, the closest distance between Ile^{23} and cholesterol is 5.9 Å with the side chains of the cholesterol molecules extending between residues Trp^{98} and Val^{108} toward the surface of the protein (Fig. 5). This finding supports the notion that Ile^{23} interactions with the protein may help stabilize Ile^{20} in an orientation where it can form positive van der Waal contacts with the cholesterol molecule and that Ile^{23} does not interact directly with the cholesterol molecule. However, it should be kept in mind that the cholesterol side chain is flexible and conformations other than what are seen in Fig. 5 could be possible.

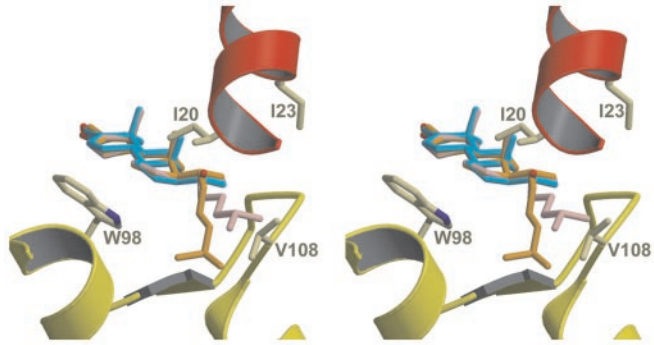

FIG. 5. **Superposition of cholesterol from the structures of β-cryptogein (*pink*) and the ligand binding domain of retinoic acid-related orphan receptor α (*orange*) onto the like atoms of pregnenolone (*light blue*) bound to SULT2B1b.** Residues Ile^{20} and Ile^{23} (*khaki*) from the amino-terminal helix (*red*) that have been shown to be important for cholesterol binding specificity are also shown. The cholesterol side chains are found positioned in a groove between Trp^{98} and Val^{108} extending toward the surface of the protein. This is away from Ile^{23} but is still close to Ile^{20}. Superposition is based on the 20 structurally equivalent atoms not in the side chain. The r.m.s. deviation values of cholesterol to pregnenolone from the β-cryptogein and ligand binding domain of retinoic acid-related orphan receptor α structures are 0.20 and 0.25 Å, respectively. This figure was created using MOLSCRIPT and Raster3D (31, 32).

In conclusion, these structures reveal a different catalytic binding orientation of the acceptor substrate than previously seen and provide insight into the role the amino terminus plays in dictating substrate specificity for cholesterol between the SULT2B1a and SULT2B1b proteins. In addition, these structures combined with previous structures of other cytosolic sulfotransferases help us to understand better the broad overlapping substrate specificities of these enzymes.

Acknowledgments—We thank Dr. J. Krahn and Dr. T. Hall for careful reading of the paper. Data for the pregnenolone-bound data set were collected at Southeast Regional Collaborative Access Team 22-ID beamline at the Advanced Photon Source, Argonne National Laboratory. Supporting institutions may be found at www.ser.anl.gov/new/members.html. Use of the Advanced Photon Source was supported by the U. S. Department of Energy, Basic Sciences, Office of Science under contract number W-31–109-Eng-38.

REFERENCES

1. Coughtrie, M. W., Sharp, S., Maxwell, K., and Innes, N. P. (1998) *Chem. Biol. Interact.* **109,** 3–27
2. Falany, C. N. (1997) *FASEB J.* **11,** 206–216
3. Strott, C. A. (2002) *Endocr. Rev.* **23,** 703–732
4. Her, C., Wood, T. C., Eichler, E. E., Mohrenweiser, H. W., Ramagli, L. S., Siciliano, M. J., and Weinshilboum, R. M. (1998) *Genomics* **53,** 284–295
5. Fuda, H., Lee, Y. C., Shimizu, C., Javitt, N. B., and Strott, C. A. (2002) *J. Biol. Chem.* **277,** 36161–36166
6. Kuroki, T., Ikuta, T., Kashiwagi, M., Kawabe, S., Ohba, M., Huh, N., Mizuno, K., Ohno, S., Yamada, E., and Chida, K. (2000) *Mutat. Res.* **462,** 189–195
7. Jetten, A. M., George, M. A., Nervi, C., Boone, L. R., and Rearick, J. I. (1989) *J. Invest. Dermatol.* **92,** 203–209
8. Kawabe, S., Ikuta, T., Ohba, M., Chida, K., Ueda, E., Yamanishi, K., and Kuroki, T. (1998) *J. Invest. Dermatol.* **111,** 1098–1102
9. Hanley, K., Wood, L., Ng, D. C., He, S. S., Lau, P., Moser, A., Elias, P. M., Bikle, D. D., Williams, M. L., and Feingold, K. R. (2001) *J. Lipid Res.* **42,** 390–398
10. Geese, W. J., and Raftogianis, R. B. (2001) *Biochem. Biophys. Res. Commun.* **288,** 280–289
11. Shimizu, C., Fuda, H., Yanai, H., and Strott, C. A. (2003) *Endocrinology* **144,**

1186–1193
12. Baulieu, E. E., Robel, P., and Schumacher, M. (2001) *Int. Rev. Neurobiol.* **46,** 1–32
13. Alomary, A. A., Fitzgerald, R. L., and Purdy, R. H. (2001) *Int. Rev. Neurobiol.* **46,** 97–115
14. Engel, S. R., and Grant, K. A. (2001) *Int. Rev. Neurobiol.* **46,** 321–348
15. Plassart-Schiess, E., and Baulieu, E. E. (2001) *Brain Res. Brain Res. Rev.* **37,** 133–140
16. Mellon, S. H., and Vaudry, H. (2001) *Int. Rev. Neurobiol.* **46,** 33–78
17. Otwinowski, Z., and Minor, V. (1997) *Methods Enzymol.* **276,** 307–326
18. Navaza, J. (1994) *Acta Crystallogr. Sec. A* **50,** 157–163
19. Bailey, S. (1994) *Acta Crystallogr. Sec. D* **50,** 760–763
20. Pedersen, L. C., Petrotchenko, E. V., and Negishi, M. (2000) *FEBS Lett.* **475,** 61–64
21. Jones, T. A., Zou, J. Y., Cowan, S. W., and Kjeldgaard, M. (1991) *Acta Crystallogr. Sec. A* **47,** 110–119
22. Brünger, A. T. (1992) *X-PLOR: A System for X-ray Crystallography and NMR*, Version 3.1, Yale University, New Haven, CT
23. Laskowski, R. A., MacArthur, M. W., Moss, D. S., and Thornton, J. M. (1993) *J. Appl. Crystallogr.* **26,** 283–291
24. Pedersen, L. C., Petrotchenko, E., Shevtsov, S., and Negishi, M. (2002) *J. Biol. Chem.* **277,** 17928–17932
25. Rehse, P. H., Zhou, M., and Lin, S. X. (2002) *Biochem. J.* **364,** 165–171
26. Kakuta, Y., Pedersen, L. G., Pedersen, L. C., and Negishi, M. (1998) *Trends Biochem. Sci.* **23,** 129–130
27. Kakuta, Y., Pedersen, L. G., Carter, C. W., Negishi, M., and Pedersen, L. C. (1997) *Nat. Struct. Biol.* **4,** 904–908
28. Kakuta, Y., Petrotchenko, E. V., Pedersen, L. C., and Negishi, M. (1998) *J. Biol. Chem.* **273,** 27325–27330
29. Lascombe, M. B., Ponchet, M., Venard, P., Milat, M. L., Blein, J. P., and Prange, T. (2002) *Acta Crystallogr. Sec. D Biol. Crystallogr.* **58,** 1442–1447
30. Kallen, J. A., Schlaeppi, J. M., Bitsch, F., Geisse, S., Geiser, M., Delhon, I., and Fournier, B. (2002) *Structure* **10,** 1697–1707
31. Kraulis, P. J. (1991) *J. Appl. Crystallogr.* **24,** 946–950
32. Merritt, E. A., and Bacon, D. J. (1997) *Methods Enzymol.* **277,** 505–524